# Filamentation of the surface plasma layer during the electrical explosion of conductors in strong magnetic fields

V. Oreshkin, S. Chaikovsky, I. Datsko, N. Labetskaya, E. Oreshkin, N. Ratakhin, A. Rousskikh, V. Vankevich, Alexandre Chuvatin

# Filamentation of the Surface Plasma Layer during the Electrical Explosion of Conductors in Strong Magnetic Fields

V. I. Oreshkin[1,2], S. A. Chaikovsky[1,3,4], I. M. Datsko[1], N. A. Labetskaya[1], E. V. Oreshkin[4,a)], N. A. Ratakhin[1,4], A. G. Rousskikh[1], V. A. Vankevich[1] and A.S. Chuvatin[5,6]

[1]Institute of High Current Electronics, Siberian Branch, RAS, 634055 Tomsk, Russia

[2]National Research Tomsk Polytechnic University, 634050 Tomsk, Russia

[3]Institute of Electrophysics, Ural Branch, RAS, 620016 Ekaterinburg, Russia

[4]Lebedev Physical Institute, RAS, 119991 Moscow, Russia

[5]Ecole Polytechnique, 91128 Palaiseau, France

[6]Sorbonne Université, 75005 Paris, France.

[a)]Author to whom correspondence should be addressed: Oreshkin@lebedev.ru

*A model has been considered to describe the development of a surface discharge over a conductor electrically exploding in a strong magnetic field. A simulation performed using this model has shown that in the initial stage of the conductor explosion, a plasma layer several tens of micrometers thick with an electron temperature of several electronvolts is formed on the metal surface. Based on the theory of small perturbations, the development of thermal filamentation instabilities that form in the surface plasma layer has been analyzed. The characteristic growth rates and wavelengths of these instabilities have been determined. The theoretical results were compared with the results of experiments performed on the ZEBRA generator (providing load currents of amplitude about 1 MA and rise time about 100 ns) and on the MIG generator (providing load currents of amplitude about 2 MA and rise time about 100 ns). For the conditions implemented with these generators, the filamentation model gives rise times of thermal filamentation instabilities of tens of nanoseconds at characteristic wavelengths of the order of 100 μm. These values are in good agreement with experimental data, which indicates the adequacy of both the surface discharge development model and the filamentation model.*

## Introduction

There are various applications of the electrical explosion of conductors (EEC) in a strong magnetic field. One of the most important applications of such an explosion mode is the implementation of potential inertial confinement fusion (ICF) schemes within the framework of the MagLIF (Magnetized Liner Inertial Fusion [1-3]) concept, in which the compression of an

initially heated deuterium-tritium mixture by a metal liner is supposed to be used. To implement the ICF in the MagLIF concept, as well as in other schemes that use Z pinches, more powerful current generators capable of producing currents of amplitude at least 50 MA are required [4-6]. At this level of current, the electromagnetic energy density in the load area is so high that a surface explosion of the transmission line electrodes may occur, leading to a decrease in the proportion of energy transferred to the load. Related to this is another reason for interest in such an EEC mode, namely, the need to provide efficient electromagnetic energy transfer in magnetically isolated lines in the presence of megagauss fields. Other important applications in which this EEC mode is implemented are, first, the generation of strong magnetic fields, both by compression of metal shells [7,8] and by exploding single-turn solenoids [9]; second, the electromagnetic acceleration of bodies, such as the acceleration of metal plates in experimental studies of shock waves [10-12]; third, the compression of heavy metal liners, in which extreme states with pressures of $10^{11}$–$10^{13}$ Pa can be attained [8,13], etc.

The main processes occurring during an EEC in a fast-rising megagauss magnetic field [14-18] are a shock wave and a nonlinear diffusion wave of the magnetic field, the formation of a dense low-temperature plasma, and the development of various types of large-scale instabilities. The rate of nonlinear diffusion is anomalously high compared to the usual rate of penetration of an electromagnetic field into a conductor. The increase in the diffusion rate is associated with a decrease in the electrical conductivity of the metal due to its heating by the flowing current. Nonlinear diffusion may occur only if the magnetic field is strong enough [8,17], that is, if its induction is greater than

$$B_0 \approx \sqrt{\frac{8\pi}{\beta_T}}, \tag{1}$$

where $\beta_T = \frac{1}{\delta_{met}^0 \rho_{met}^0 c_v} \frac{\partial \delta}{\partial T}$, $\delta_{met}^0$ and $\rho_{met}^0$ are the metal resistivity and density at 273 K, $c_v$ is the heat capacity at constant volume, and $\frac{\partial \delta}{\partial T}$ is the temperature derivative of the metal resistivity. The magnetic field induction $B_0$ is several tens of Teslas for the majority of metals (36.5 T for aluminum). This value of magnetic induction corresponds to a magnetic pressure on the conductor surface of about $10^9$ Pa. Therefore, the nonlinear diffusion wave propagates through the material together with the shock wave caused by the pressure of the magnetic field on the conductor surface.

An electrical explosion of conductors is usually accompanied by the development of various types of instabilities. These can be both thermal instabilities, which manifest themselves as strata [18-20], and Rayleigh–Taylor instabilities, the growth of which is accompanied by

plasma ejection across the magnetic field lines [21]. These types of instabilities develop rather late in the explosion, when the conductor material is heated to high temperatures. One more type of instabilities, which develop at an earlier stage of the explosion, was observed in experiments described in [15,22]. In these experiments, bright spots were observed on the conductor surface at the stage preceding the explosion. At a later stage, the surface was covered with filaments, that is, with plasma entities stretched along the direction of current flow. It seems likely that these filaments were current channels that carried part of the total current through the load. With a further increase in current, the filaments disappeared, and the conductor surface underwent stratification.

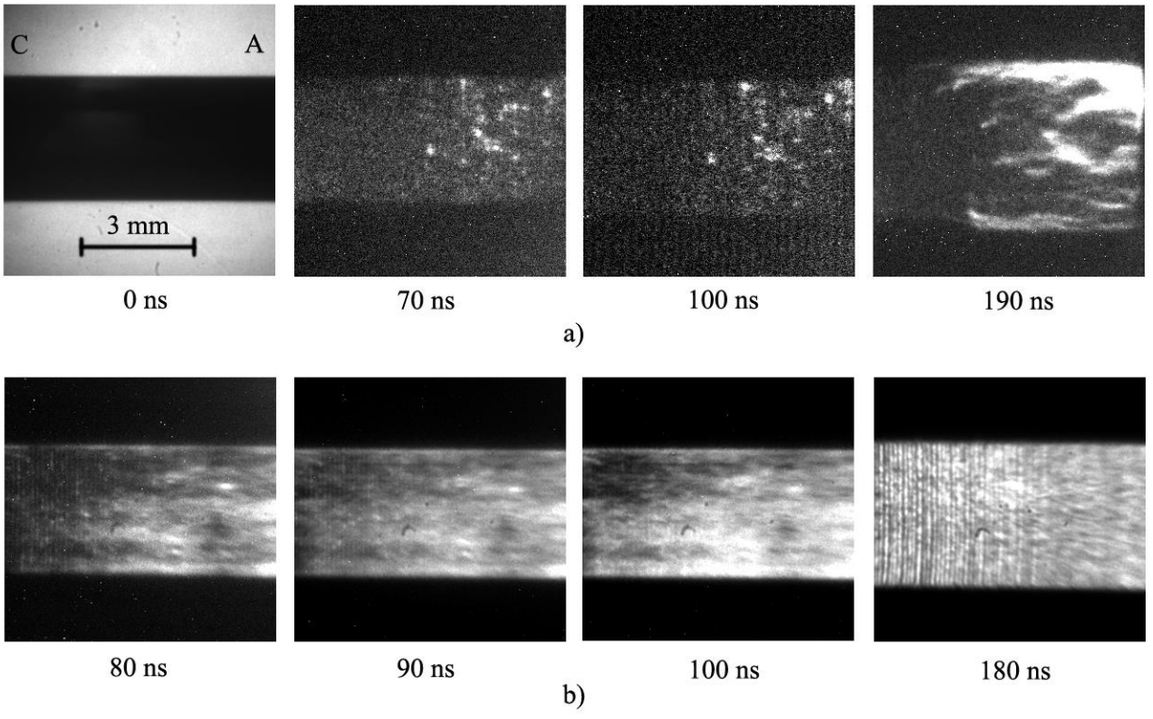


Fig. 1. Images of an exploded duralumin conductor of initial diameter 3 mm taken in the visible radiation range at various times from the onset of current flow ($t$ = 0) at a generator current of amplitude 1.3 MA and rise time 100 ns (a) and of amplitude 2.0 MA and rise time 100 ns (b). The first frame in Fig. 1a is a visible backlighting image taken prior to the shot; C and A mark the cathode and anode, respectively. [IM Datsko, NA Labetskaya, SA Chaikovsky, VA Van'kevich1 and VI Oreshkin, Journal of Physics: Conference Series, Vol. 2064, Article ID 012012, 2021; licensed under a Creative Commons Attribution (CC BY) license].

This is illustrated by Fig. 1, which shows photos of exploded aluminum conductors of diameter 3 mm and length about 1 cm [22]. The experiment was performed on the MIG generator providing a current through the load of amplitude up to 2 MA and rise time about 100

ns [16,23]. A more thorough experimental study was carried out on the ZEBRA generator [15], which provided a current pulse through the load of amplitude about 1 MA and rise time about 100 ns. In the latter experiment, aluminum conductors of diameter 1 mm and length 7 mm were exploded. Bright spots were detected at a load current of about 300 kA, when the magnetic field induction on the conductor surface reached about 120 T, that is, it was three to four times higher than $B_0$. The spots were about 5 μm in size (the minimum size was determined by the resolution of the recording equipment), and their number reached 500 $mm^{-2}$. Filaments appeared 10–15 ns after the detection of the bright spots at a load current of about 400 kA. The distance between individual filaments was 50–100 μm.

The most probable reason for the appearance of filaments observed as separate current channels in the current-carrying plasma layer was the development of thermal instabilities. The growth of thermal instabilities in a plasma is determined by the nature of the temperature dependence of resistivity [18,24]. If the resistivity of a material increases with temperature, as is the case, for example, of a liquid metal, the thermal instabilities lead to the formation of strata [19,25,26], that is, layers normal to the current flow direction. In the opposite case, when the resistivity decreases with increasing temperature, as is the case of a high-temperature plasma, the development of thermal instabilities should lead to the formation of individual current channels [27-30]. In this paper, the development of filament instabilities of the surface plasma layer formed during the explosion of metal conductors in strong magnetic fields is analyzed based on a theory of small perturbations. Section II presents a model which describes the development of a surface discharge during the explosion of conductors in strong magnetic fields based on the theory of ectons [31]. The results of a magnetohydrodynamic simulation of the explosion of conductors in strong magnetic fields are given in Section III. In Section IV, a model of the linear stage of development of filament instabilities is constructed and an analysis of the growth of these instabilities, their characteristic wavelengths, and their growth rates is performed.

## 1. A model of the surface discharge developing over a conductor exploding in a strong magnetic field

From our point of view, the most probable reason for the appearance of bright spots on the surface of an exploding conductor is the formation of ectons [31]. Ectons are plasma-producing centers formed on a cathode in the process of explosive emission, which is caused by the electrical explosion of metal microprotrusions [32]. Explosive electron emission occurs only at high electric field strengths on the cathode surface and is accompanied by a fast heating of the metal in microvolumes [32,33]. As shown in [31], electrons are emitted in the form of individual bunches, named ectons. The appearance of an ecton is associated with overheating of the metal

during a microexplosion, and the termination of its operation is due to the cooling of the emission zone [33]. The operation of an ecton is a complex and multifactor process, the details of which are still not clearly understood. In addition to the emission of electrons, the ecton operation is accompanied by the generation of multiply charged ions, liquid metal drops, and the like, and after the end of the process, micrometer-size craters usually remain on the cathode surface [31,33].

Let us analyze the process of formation of a plasma layer on the surface of a conductor in a rapidly growing magnetic field. Consider a cylindrical metal rod of radius $R_{Rod}$ and length $l$, surrounded by a return conductor of radius $R_{Rc}$ (Fig. 2). Assume that a current increasing in time flows along the rod in the direction opposite to the direction of the $z$ axis. Note that the geometry of the problem shown in Fig. 1 coincides with that of coaxial vacuum transmission lines [34,35].

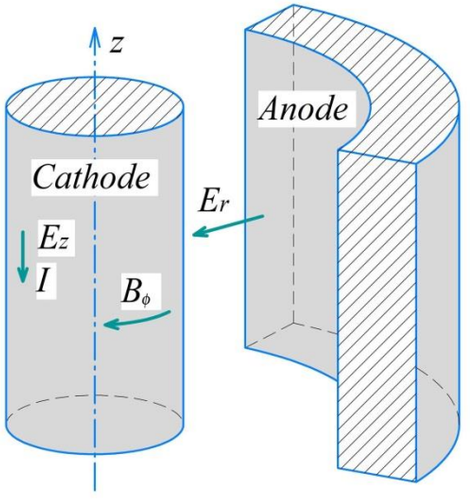


Fig. 2. Pattern of electric and magnetic fields.

Let us estimate the possibility of explosive emission developing on the surface of a conductor in a fast-rising magnetic field. For explosive emission to be initiated, the electric field strength on the cathode surface must reach several hundreds of kilovolts per centimeter [34,35]. In our situation, a radial electric field arises between the metal rod and the return conductor. Let $U$ be the potential difference between the rod and the return conductor. Then the value of the radial component of the electric field strength on the rod surface can be estimated as

$$E_r \approx \beta \frac{U}{R_{Rc} - R_{Rod}}, \tag{2}$$

where $\beta$ is the enhancement factor for the field strength at the rod surface relative to the average field strength in the electrode gap. The value of the field enhancement factor can be determined from the equation $\nabla \mathbf{E} = 0$, which holds for an electrode gap. From this equation it follows that $E_r \propto \frac{const}{r}$, and then we may write the following expression for the field enhancement factor:

$$\beta = \left( \frac{R_{Rc}}{R_{Rod}} - 1 \right) \left( \ln \frac{R_{Rc}}{R_{Rod}} \right)^{-1}. \tag{3}$$

The potential difference between the rod and the return conductor can be estimated as [34,35]

$$U \approx \frac{1}{c^2} L \frac{\partial I}{\partial t}, \tag{4}$$

where $L = 2l \ln \frac{R_{Rc}}{R_{Rod}}$ is the inductance of the rod–return-conductor system and $c$ is the velocity of light in vacuum. Then, substituting expressions (3) and (4) in expression (2), we can estimate the radial component of the electric field on the rod surface as

$$E_r \approx \frac{2l}{c^2 R_{Rod}} \frac{dI}{dt}. \tag{5}$$

For the experiments performed on the ZEBRA and MIG generators, the current rise rate $dI/dt$ can be estimated as $10^{13}$ A/s. Then for $\frac{l}{R_{Rod}} \approx 10$ the radial electric field strength should be no less than 200 kV/cm. For such electric field strength on the surface of a rod conductor, explosive electron emission should occur, that is, if the conductor would explode in a strong field, explosive emission centers should form on its surface.

Next, we estimate the parameters of the plasma layer formed during the operation of explosive emission centers, while following the methodology described in [36]. The explosion of cathode microprotrusions during explosive emission was studied in many works [18,34,37-39]. According to the data given in [37,38], when one microprotrusion explodes, the (initially solid) metal of volume 1–2 μm$^3$ goes into a plasma with a temperature of several electronvolts; that is, one ecton produces (1–2)·$10^{11}$ metal ions. As the number of ectons $N_{ect}$ is 200–500 mm$^2$ [15], the total number of ions formed during explosive electron emission, $N_i$ can be estimated as (0.5–1)·$10^{16}$ cm$^{-2}$. In addition to these ions, the surface layer must contain molecules of gases desorbed from the conductor surface. The number of these molecules is of the order of $10^{15}$ cm$^2$ [18], which is comparable to the number of ions formed in the process of explosive emission.

These estimates correlate with experimental data on vacuum arc discharges. In a vacuum arc, the number of metal ions formed in explosive emission centers is comparable to the number of ions of desorbed gases, and the electron temperature is several electronvolts [40].

Apparently, the formation of a current sheath on the conductor surface does not occur immediately after the explosion of microprotrusions, since the plasma bunches formed during the explosion of individual ectons must merge to form connected regions. The ectons are spaced $\left(N_{ect}\right)^{-1/2} \approx$ 40–70 μm. The ecton plasma, expanding with a thermal velocity of the order of $10^6$ cm/s, should cover this spacing in 5–10 ns. However, in a magnetic field, the plasma can freely expand only along the magnetic field lines, that is, along the azimuthal direction [15]. Its expansion across the magnetic field lines, along the *z* and *r* directions, is difficult, so the formation of a connected region should be delayed.

Let us estimate the current that flows in the surface plasma layer. We will proceed from the following considerations. First, the fraction of the current flowing in the layer is small, that is, almost the entire generator current flows through the metal rod. Second, there are no skin effects in the surface layer due to its small thickness. Therefore, both the azimuthal magnetic field $B_\varphi$ and the axial electric field $E_z$ in the surface layer will be determined by the current flowing through the rod. The specific form of the time dependence of $E_z$ will be determined in the next section using a magnetohydrodynamic simulation of the conductor explosion process.

Next, it can be assumed that the rate of change in the thickness of the surface plasma layer is small compared with the thermal velocity of the plasma, since it is confined by the pressure of the magnetic field. In this case, the following equilibrium condition can be written for the plasma layer:

$$\frac{\partial p_{pl}}{\partial r} \approx \frac{1}{c} j_z^{pl} B_\varphi , \qquad (6)$$

where $p_{pl} = (1+Z)kT\frac{N_i}{\Delta_{pl}}$ is the thermal pressure in the surface plasma layer of thickness $\Delta_{pl}$, $Z$ is the average ion charge, $T$ is the plasma temperature in the layer, $k$ is Boltsmann's constant, $j_z^{pl} \approx \frac{I_{pl}}{2\pi R_{Rod}\Delta_{pl}}$ is the plasma density in the layer, $I_{pl}$ is the current flowing through the plasma layer, $B_\varphi \approx \frac{2I}{cR_{Rod}}$ is the magnetic field induction in the layer, and $I$ is the current flowing through the metal rod (it is assumed that $I_{pl} << I$).

Then the equilibrium condition (6) becomes

$$(1+Z)kTN_i \approx \frac{1}{c^2}\frac{\Delta_{pl}}{\pi R_{Rod}^2} I_{pl} I \,. \tag{7}$$

On the other hand, for the plasma layer, Ohm's law can be written as

$$E_z = j_{pl}\delta_{pl} = \frac{I_{pl}}{2\pi R_{Rod}\Delta_{pl}}\delta_{pl}, \tag{8}$$

where $E_z$ is the electric field strength; $j_{pl}$ and $\delta_{pl}$ are, respectively, the current density in the plasma layer and its resistivity. Since the magnetic field is directed along the azimuth and the current flows along the z axis, the resistivity (across the field) is given by the expression [41]

$$\delta_{pl} = \frac{m_e}{e^2 n_e \tau_e} = \frac{4\sqrt{2\pi}}{3}\frac{e^2\sqrt{m_e}Z\Lambda}{(kT)^{3/2}}, \tag{9}$$

where $n_e$ is the electron density; $\tau_e$ is the electron-ion collision time; $e$ and $m_e$ are the electron charge and mass, respectively, and $\Lambda$ is the Coulomb logarithm. For a plasma temperature of 3–5 eV, an average charge of three to five, and $\Lambda$=10, the plasma layer resistivity $\delta_{pl}$ can be estimated as 0.05–0.06 Ω·cm.

As a result, from expressions (7) and (8), we obtain expressions that determine the thickness of the surface plasma layer and the magnitude of the current flowing through the plasma layer:

$$\Delta_{pl} \approx \sqrt{0.5c^2(1+Z)kTN_i\frac{R_{Rod}\delta_{pl}}{E_z I}} \,. \tag{10}$$

$$I_{pl} \approx \sqrt{2\pi^2 c^2(1+Z)kTN_i\frac{E_z R_{Rod}^3}{\delta_{pl} I}}; \tag{11}$$

Expressions (10) and (11) involve the electric field strength $E_z$. The time dependence of $E_z$ depends on a whole complex of nonlinear processes that accompany the explosion of a conductor in a strong magnetic field. The forms of this dependence will be determined in the next section using a magnetohydrodynamic simulation of the conductor explosion process.

## 2. Magnetohydrodynamic simulation of the explosion of aluminum conductors

The process of the explosion of aluminum conductors was simulated using the EXWIRE one-dimensional magnetohydrodynamic code [42]. The simulation did not take into account the effects associated with the formation of a surface plasma layer described in the previous section. The system of equations implemented in the EXWIRE code included hydrodynamic equations and Maxwell's equations. For the cylindrical case, the system of equations was written in Lagrangian coordinates as

$$\frac{d\rho}{dt}+\frac{\rho}{r}\frac{\partial v}{\partial r}=0 \ ; \tag{12}$$

$$\rho\frac{dv}{dt}=-\frac{\partial p}{\partial r}-j_z B_\varphi ; \tag{13}$$

$$\rho\frac{d\varepsilon}{dt}=-\frac{p}{r}\frac{\partial v}{\partial r}+\frac{j_z^{\,2}}{\sigma}+\frac{1}{r}\frac{\partial}{\partial r}(\kappa\frac{\partial T}{\partial r}); \tag{14}$$

$$\frac{1}{c}\frac{\partial B_\varphi}{\partial t}=\frac{\partial E_z}{\partial r} \ ; \ j_z=\frac{c}{4\pi r}\frac{\partial (rB_\varphi)}{\partial r} \ ; \tag{15}$$

$$j_z == \sigma E_z ; \tag{16}$$

$$\varepsilon = f(\rho,T); \quad p=f(\rho,T) \tag{17}$$

where $\frac{d}{dt}=\frac{\partial}{\partial t}+v\frac{\partial}{\partial r}$ is the substantial derivative; $\rho$ and $T$ are the material density and temperature, respectively; $v$ is the radial velocity of the material; $p$ and $\varepsilon$ are the pressure and internal energy, respectively; $B_\varphi$ is the azimuthal component of the magnetic field strength; $E_z$ is the axial component of the electric field strength; $j_z$ is the axial component of the current density; $\kappa$ and $\sigma=1/\delta$ are the thermal conductivity of the metal and its electrical conductivity (reciprocal of the resistivity), respectively.

The system of MHD equations (12)–(16) is closed by the equations of state of matter (17). For the metal, we used wide-range semi-empirical equations of state [43] obtained on the basis of the model proposed in [44], which take into account the effects of high-temperature melting and evaporation. The electrical conductivity of aluminum was determined using the tables [45] compiled by M. Desjarlais at Sandia National Laboratories, USA, and the model proposed in [46] and modified taking into account experimental data.

The boundary conditions for the system of equations (12)–(16) were set as follows: for equation (13): $p = 0$ at $r = R_{Rod}$ and $\frac{\partial p}{\partial r} = 0$ at $r = 0$; for equations (14): $\frac{\partial T}{\partial r} = 0$ at $r = R_{Rod}$ and $r = 0$, and for Maxwell's equations (16): $B_\varphi = 0$ at $r = 0$ and $B_\varphi = \frac{2I}{cR_{Rod}}$, where $I$ is the current flowing through the conductor, at $r = R_{Rod}$. In the calculations, the following time dependence of current was used: $I(t) = I_0 \sin\left(\frac{\pi}{2}\frac{t}{\tau_f}\right)$, where $I_0$ is the current amplitude and $\tau_f$ is the current rise time. Calculations were performed for an aluminum conductor in two variants: 1 mm in diameter, $I_0$ = 1 MA, and $\tau_f$ = 100 ns, and 3 mm in diameter, $I_0$ = 2 MA, and $\tau_f$ = 100 ns. In the first and second variants, the conditions close to those of the experiments on ZEBRA and MIG facilities, respectively, were simulated.

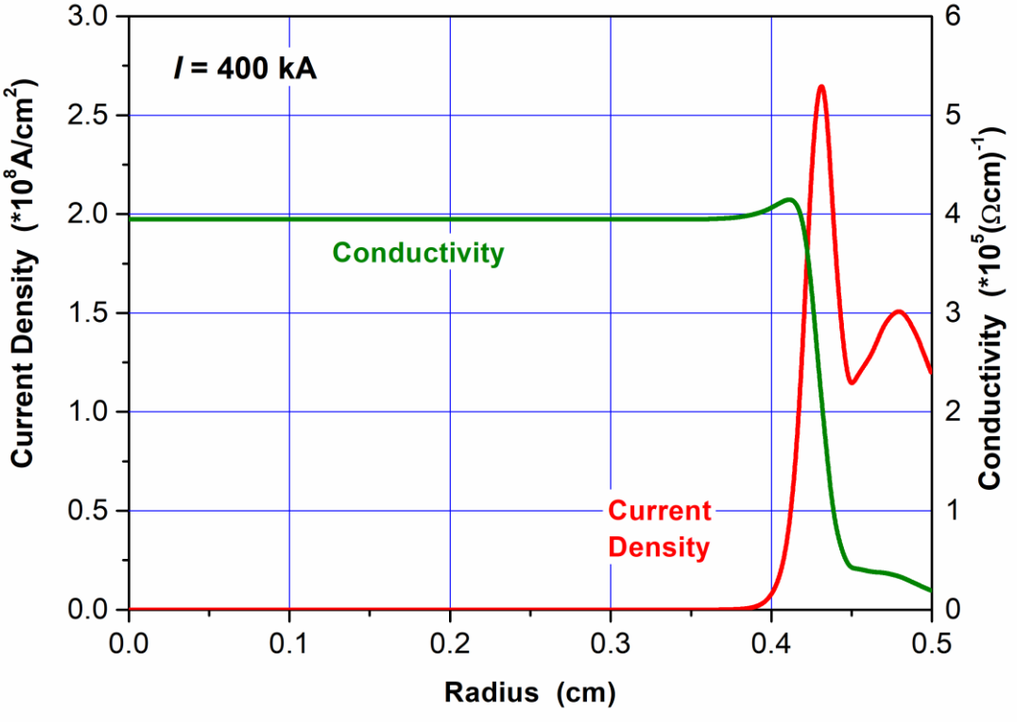


(a)

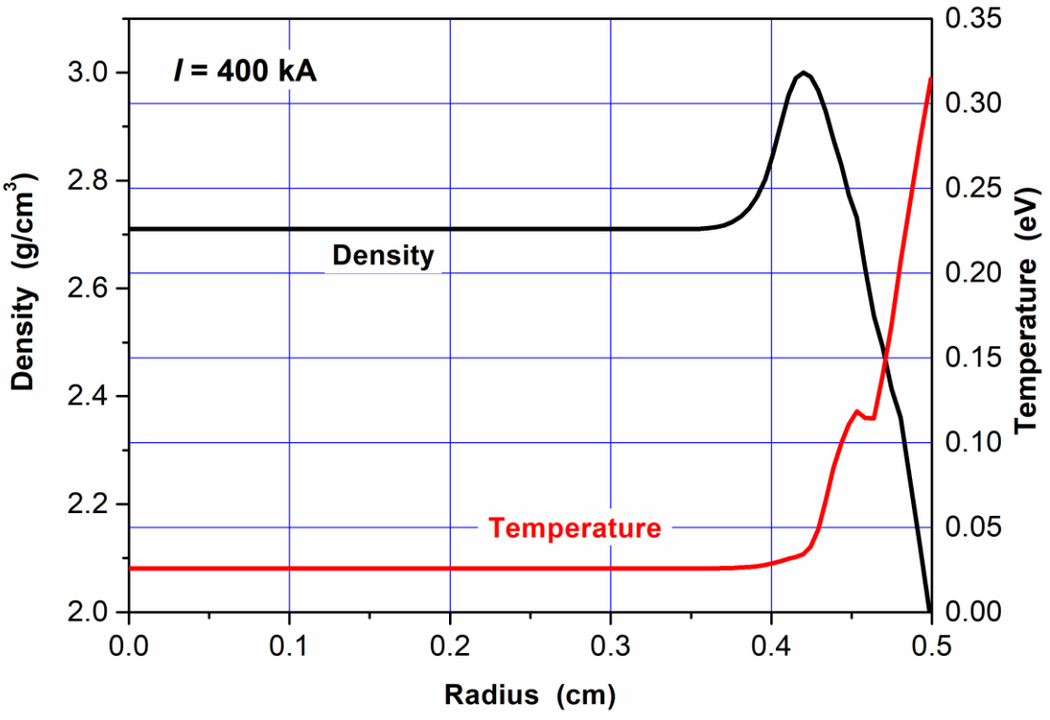


(b)

Fig. 3. Results of the MHD simulation of the explosion of an aluminum conductor 1 mm in diameter showing the distributions of the metal conductivity and current density (a) and of the material density and temperature (b).

As already noted, the electrical explosion of a conductor in a magnetic field the induction of which is greater than $B_0$ is accompanied by a non-linear diffusion wave (NDW) of the magnetic field and a shock wave (SW) propagating in the metal [47,48]. Nonlinear diffusion is characterized by an anomalously high penetration rate of the electromagnetic field into the conductor compared with ordinary diffusion. The increase in the diffusion rate is associated with a decrease in the electrical conductivity of the metal due to its heating by the flowing current. The velocity of the nonlinear diffusion wave is determined by the velocity of propagation of the current density maximum into the bulk conductor. This can be seen in Fig. 3, which shows the radial distributions of various parameters for the first variant (conductor diameter = 1 mm, $I_0$ = 1 MA, $\tau_f$ = 100 ns) at the time when the current through the conductor reaches 400 kA (27 ns from the onset of current flow), that is, approximately at the time when filaments were observed on the surface of the exploding conductor in experiments on the ZEBRA facility [15]. As can be

seen from this figure, an NDW and an SW have formed and propagate into the bulk conductor when filaments already exist in the surface plasma layer according to the experiment. At this time, the surface temperature of the conductor reaches 0.3 eV; that is, the metal in the surface layer of the rod passes into a liquid state.

The nonlinear processes associated with the NDW and SW propagation significantly affect the exploding conductor resistance and the axial electric field, as can be seen from Fig. 4. This figure shows the time dependences of the current $I(t)$, axial electric field strength on the conductor surface, $E_z(t)$, and conductor resistance $Z(t)= E_z(t)/I(t)$ for two variants in which the explosion conditions were simulated for experiments performed on the ZEBRA generator (see Fig. 4a) and on the MIG generator (see Fig. 4b). We see that in the initial stage of the explosion, the resistance of the conductor decreases with time. This is due to the increase in the thickness of the skin layer, which can be estimated as $\Delta_{sk} \approx c\sqrt{\frac{\delta_{met}^0 t}{4\pi}}$ [49]. When the induction of the magnetic field on the conductor surface reaches value $B_0$, the diffusion of the magnetic field goes into a nonlinear mode. At this time, the conductor resistance $Z(t)$ falls to a minimum. In the nonlinear mode, the resistance is determined by two opposing factors. The first factor, leading to a decrease in resistance, is an increase in the size of the region in which current flows (behind the NDW front). The second factor, leading to an increase in resistance, is a decrease in metal conductivity behind the NDW front. As a result, as can be seen from Fig. 4, at the nonlinear stage $Z(t)$ slightly increases with time.

The plots shown in Fig. 4 allow us to estimate the electric field strength on the conductor surface during the formation of the plasma layer and the development of filaments. For conditions approximately corresponding to the experiments on the ZEBRA generator (see Fig. 4a) and on the MIG generator (see Fig. 4b), the field strength $E_z$ in this time interval is 3–6 kV/cm and about half that, respectively. Note that the estimates of the values of the axial electric field, made without taking into account the effect of nonlinear diffusion of the magnetic field in [36], give 2–3 times smaller values of $E_z$. With the field strength known, we can estimate the thickness of the plasma surface layer $\Delta_{pl}$ and the current flowing through the layer, $I_{pl}$, using expressions (10) and (11) obtained in the previous section. For the estimation, we assume (see the previous section) that $N_i \approx$ (0.5–1)·$10^{16}$ cm$^{-2}$ and the resistivity $\delta_{pl} \approx 0.05$–$0.06$ Ω·cm, which corresponds to a plasma temperature of 3–5 eV and an average charge of 3–5. Then, for the ZEBRA generator conditions [15], in view of the total current through the conductor $I \approx$ 300–400 kA, we obtain the plasma surface layer thickness $\Delta_{pl} \approx 40$–$50$ μm and the current

flowing through the layer $I_{pl} \approx 100$–$200$ A. For the MIG generator conditions [22], we have $I \approx$ 600–800 kA and, respectively, $\Delta_{pl} \approx 60$–$90$ μm and $I_{pl} \approx 200$–$500$ A.

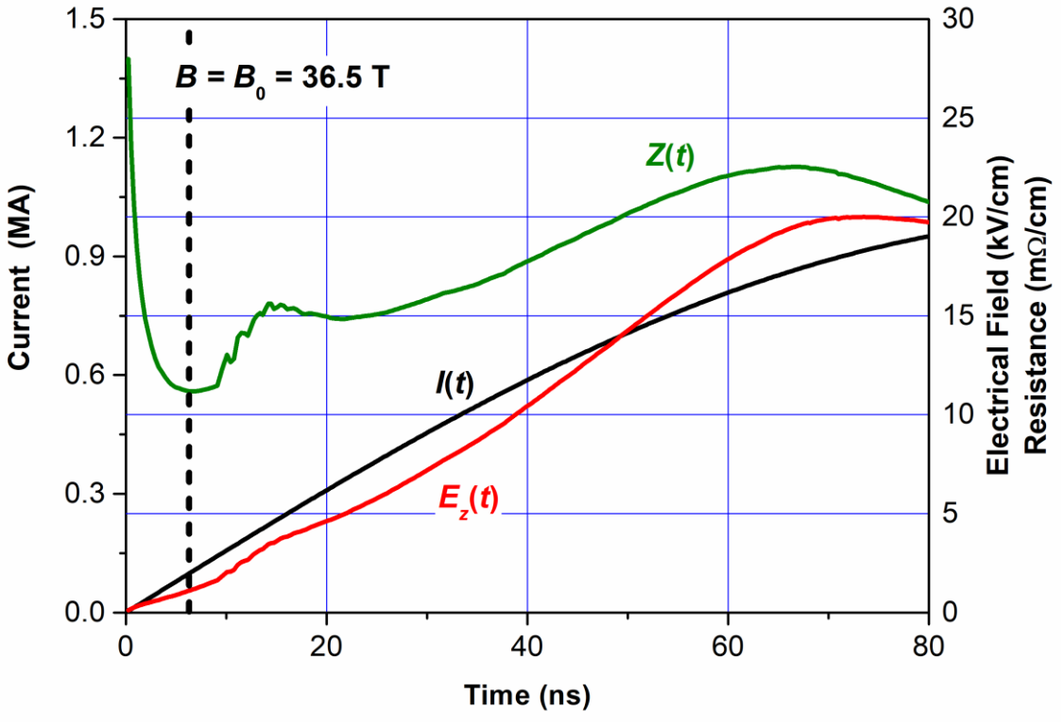


(a)

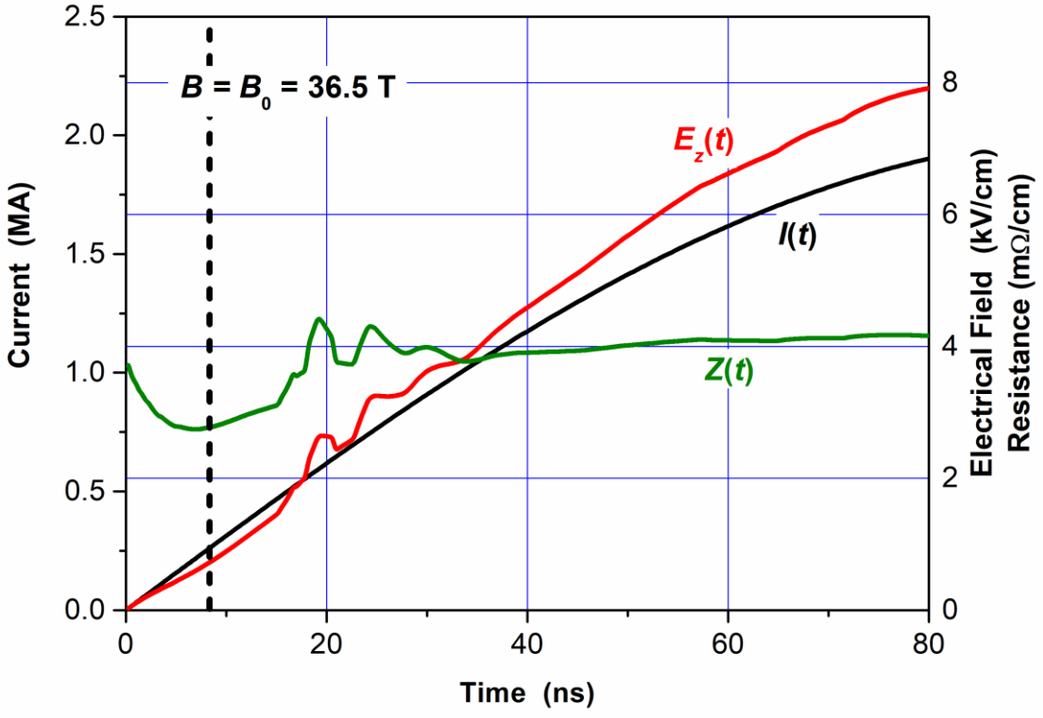


(b)

Fig. 4. Results of the MHD simulation of the explosion of aluminum conductors 1 mm in diameter at $I_0$ = 1 MA and $\tau_f$ = 100 ns (a) and 3 mm in diameter at $I_0$ = 2 MA, and $\tau_f$ = 100 ns (b).

Thus, in both cases, at the initial stage of the electrical explosion of a conductor in a skinned current mode, a plasma layer of thickness several tens of micrometers forms on the metal surface. The ion density in this layer is close in order of magnitude to $10^{18}$ cm$^{-3}$. Only a small (hundredths of a percent) part of the total load current flows through this layer. The current density in the plasma layer, $j_z^{pl} = \dfrac{I_{pl}}{2\pi R_{Rod}\Delta_{pl}}$, is close in order of magnitude to $10^5$ A/cm$^2$, which is three orders of magnitude less than the current density in the exploding conductor (see Fig. 3a), which is higher than $10^8$ A/cm$^2$.

## 3. Filamentation model

Filamentation instabilities, which give rise to the formation of individual current channels, are often observed in experiments with plasma focuses [27,28] and Z pinches [29,50,51]. As noted above, the most probable reason for the appearance of filaments is the development of thermal instabilities, the structure of which is determined by the nature of the dependence of the resistivity of the material on temperature and density. If the resistivity of a

material increases with temperature, as is the case for most metals in liquid and condensed states, thermal instabilities lead to the formation of layered structures (strata) in which the layers are normal to the direction of current flow [25,26]. This is observed in experiments on the electrical explosion of conductors. If the resistivity of a material decreases with increasing temperature, as is the case for high-temperature plasmas, thermal instabilities give rise to the formation of current channels (filaments) [27-30].

Let us consider the processes responsible for the formation of filaments in a cylindrical plasma shell, the thickness of which, $\Delta_{pl}$, is much less than its radius. The main equation that will be used below to analyze thermal filamentation instabilities (TFIs) is the equation describing the heating of a substance due to the Joule energy input, which we write in the following form:

$$\rho c_v \frac{\partial T}{\partial t} = \frac{E_z^2}{\delta_{pl}} - \frac{1}{r}\frac{\partial}{\partial \varphi}\left(-\frac{\kappa}{r}\frac{\partial T}{\partial \varphi}\right) \tag{18}$$

where $\rho = m_i \dfrac{N_i}{\Delta_{pl}}$ is the density of the material, $m_i$ is the ion mass, $c_v = \dfrac{3}{2}\dfrac{(1+Z)kT}{m_i}$ is the heat capacity of the plasma, and $\kappa$ is the thermal conductivity.

The problem will be considered in the following statement. Assume that in the initial state the shell is uniform (there are no temperature and density gradients in it), but over time, azimuthal nonuniformities of temperature and density may appear in it. Then for the unperturbed shell, equation (18) takes the form:

$$\rho_0 c_v \frac{\partial T_0}{\partial t} = \frac{E_z^2}{\left(\delta_{pl}\right)_0}, \tag{19}$$

where the subscript "zero" marks the values of unperturbed functions. Equation (19) is a nonstationary energy balance equation.

We assume that the temperature and density are perturbed along the azimuth and describe them as

$$T(t,\varphi) = T_0(t) + T_1(t,\varphi), \qquad \rho(t,\varphi) = \rho_0(t) + \rho_1(t,\varphi), \tag{20}$$

where $T_1(t,\varphi)$ and $\rho_1(t,\varphi)$ are the small perturbations of temperature and density, respectively. (Everywhere below we will denote the unperturbed values of functions by subscripts "0" and their small perturbations by subscripts "1"). Let us consider the case when the resistivity of a material is a function of temperature and does not depend on its density. This is true for a classical plasma, in which the resistivity is determined by expression (9), that is, it weakly depends on density, only through the Coulomb logarithm $\Lambda$. Expanding the resistivity function in a series at the point $T_0$ and truncating the series to the first term, we have

$$\delta_{pl} \approx \left(\delta_{pl}\right)_0 + \frac{\partial \delta_{pl}}{\partial T} T_1 , \tag{21}$$

where $\frac{\partial \delta_{pl}}{\partial T}$ is the temperature derivative of resistivity.

Then, using (18) in view of (19)–(21), we can write an equation for the small perturbation of temperature:

$$\rho_0 c_v \frac{\partial T_1}{\partial t} + \rho_1 c_v \frac{\partial T_0}{\partial t} = -\frac{E_z^2}{\left(\delta_{pl}\right)_0^2} \frac{\partial \delta_{pl}}{\partial T} T_1 + \frac{\kappa}{r^2} \frac{\partial^2 T_1}{\partial \varphi^2} . \tag{22}$$

To find the relationship between temperature and density perturbations, we proceed from the following considerations. If the material in a perturbed region moves at a velocity less than the thermal one, the pressure in this region levels off [29,52]; that is, in our case, the pressure gradient along the azimuth must satisfy the condition $\left(\nabla p_{pl}\right)_\varphi \approx 0$. Then, if the pressure linearly depends on temperature and density, we have the following relationship between small perturbations of density and temperature:

$$\frac{\rho_1}{\rho_0} \approx -\frac{T_1}{T_0} . \tag{23}$$

We describe a small perturbation of temperature as

$$T_1(t,\varphi) = const \cdot \exp\{\gamma t + im\varphi\}, \tag{24}$$

where $\gamma$ is the instantaneous instability growth rate and $m$ is the mode number of the azimuthal perturbation. Substitution of (24) in (22) in view of (23) yields the following expression for the instantaneous instability growth rate:

$$\gamma = -\frac{1}{\rho c_v}\left(\frac{E_z^2}{\delta_{pl}^2}\left[\frac{\partial \delta}{\partial T} - \frac{\delta_{pl}}{T}\right] + \kappa k_m^2\right), \tag{25}$$

where $k_m = \frac{m}{r}$ is the wave vector. Since small perturbations will not appear below, the subscripts "0" that marked the unperturbed values of functions and thermodynamic parameters are omitted in expression (25) and will be everywhere below.

Expression (25) is the dispersion equation for FT instabilities. For a classical plasma, as follows from (9), we have $\frac{1}{\delta_{pl}} \frac{\partial \delta_{pl}}{\partial T} = -\frac{3}{2T}$; hence, expression (25) can be rewritten as

$$\gamma = \gamma_m \left(1 - \frac{k_m^2}{k_{\max}^2}\right), \tag{26}$$

The coefficients entering into expression (26) can be considered the characteristic growth rate

$$\gamma_m = \frac{5}{2}\frac{E_z^2}{\rho c_v T \delta_{pl}} = \frac{5}{3}\frac{E_z^2}{p_{pl}\delta_{pl}} \tag{27}$$

and the maximum possible value of the wave vector

$$k_{\max} = \sqrt{\frac{5}{2}\frac{E_z^2}{\kappa T \delta_{pl}}}, \tag{28}$$

where $p_{pl} = (1+Z)kT\frac{N_i}{\Delta_{pl}}$.

As we consider only azimuthal perturbations and as the magnetic field in the plasma shell is also directed along the azimuth, expression (28) contains the coefficient of electron thermal conductivity along the magnetic field, which is given by the formula [41]:

$$\kappa = \xi(Z)\frac{n_e \tau_e k^2 T}{m_e} = \xi(Z)\frac{3}{4\sqrt{2\pi}}\frac{(kT)^{5/2}k}{\sqrt{m_e}e^4 Z\Lambda}, \tag{29}$$

where $\xi(Z)$ is a dimensionless coefficient depending on the charge $Z$ ($\xi(Z)\approx 3.16$ for $Z$ = 1, $\xi(Z)\approx 6.1$ for $Z$ = 3 and $\xi(Z)\approx 12.5$ for $Z\to\infty$), which is tabulated in [41]. Then, after substitution of (9) and (29) in (28), we have

$$k_{\max} = \sqrt{\frac{5}{2\xi(Z)}}\frac{eE_z}{kT} \approx \frac{eE_z}{kT}. \tag{30}$$

Expression (30) indicates that the value of the wave vector is determined only by the electric field strength and the temperature of the material. Note that this is true not only for the filaments developing in a plasma, but also for the strata formed during the electrical explosion of a conductor [25,26].

Using expressions (27) and (30), for the conditions of the experiments performed of the ZEBRA generator [15], we obtain that the growth time of thermal instabilities, $\sim 1/\gamma_m$, is about 10 ns, and their wavelength (the distance between individual filaments), $\sim 2\pi/k_{\max}$, is 50–100 μm for a plasma temperature of 3–5 eV. For the conditions implemented with the MIG generator [22], both the growth time of thermal instabilities and their wavelength are about twice longer. Thus, the results obtained in this section are consistent with the experimental results [15,22], which indicates the adequacy of both the surface discharge development model and the filamentation model.

## Conclusion

A model of the development of a surface discharge during the explosion of a conductor in a strong magnetic field has been considered. This model has shown that in the initial stage of the electrical explosion of a conductor in a skinned current mode, a plasma layer forms on the metal surface. The plasma electron temperature is several electronvolts and the layer thickness is several tens of micrometers. This layer carries only a small (hundredths of a percent) part of the total current flowing through the load. Therefore, the strength of the axial electric field and the value of the azimuthal component of the induction vector of the magnetic field in the surface plasma layer are determined by the processes occurring in the exploded conductor. It has been shown that the ion density in the plasma layer is close in order of magnitude to $10^{18}$ $cm^{-3}$, and the current density in the layer is close to $10^5$ $A/cm^2$, which is several orders of magnitude lower than the current density in the exploded conductor.

Based on a theory of small perturbations, the development of filament instabilities of the surface plasma layer formed during the explosion of a metal conductor in a strong magnetic field has been analyzed. It was supposed that filaments arise as a result of the development of thermal instabilities, the growth of which is determined by the nature of the dependence of resistivity on temperature. If the resistivity decreases with increasing temperature, as is the case in a plasma, the development of thermal instabilities leads to the formation appearance of individual current channels. The characteristic growth rates and wavelengths of filamentation thermal instabilities have been estimated. It has been shown that these quantities are determined by the thermodynamic parameters of the plasma layer and by the strength of the axial electric field created by the exploded conductor. To estimate the strength of the axial electric field, a magnetohydrodynamic simulation of the explosion of aluminum conductors in a skinned current mode has been performed. It has been found that in this mode, the electric field strength is several kilovolts per centimeter. The theoretical results have been compared with the results of experiments performed on the ZEBRA generator [15] (about 1 MA load current amplitude and about 100 ns current rise time) and on the MIG generator [22] (about 2 MA load current amplitude and about 100 ns current rise time). For the conditions implemented in these experiments, the filamentation model has given growth times of thermal instabilities at a level of tens of nanoseconds and the characteristic wavelengths of the order of 100 μm. These values are in good agreement with the experimental data, which indicates the adequacy of both the surface discharge development model and the filamentation model.

## Acknowledgements

The work was supported by the Russian Science Foundation (grant No. 20-19-00364).

## Data availability

The data that support the findings of this study are available from the corresponding author upon reasonable request.

## References

[1] M. R. Gomez *et al.*, Physical Review Letters **113**, 155003 (2014).
[2] D. Sinars *et al.*, Physics of Plasmas **27**, 070501 (2020).
[3] D. Yager-Elorriaga *et al.*, Nucl. Fusion **62**, 042015 (2021).
[4] W. A. Stygar *et al.*, Physical Review Special Topics-Accelerators and Beams **10**, 030401 (2007).
[5] E. Grabovski *et al.*, 2015 IEEE International Conference on Plasma Sciences (ICOPS), 15360739 (2015).
[6] N. Pereira, Matter and Radiation at Extremes **5**, 026402 (2020).
[7] A. D. Sakharov, Physics-Uspekhi **9**, 294 (1966).
[8] H. Knoepfel, *Pulsed high magnetic fields* (North-Holland, Amsterdam, 1970).
[9] S. Krivosheev, V. Titkov, and G. Shneerson, Technical Physics **42**, 352 (1997).
[10] V. E. Fortov, Physics-Uspekhi **50**, 333 (2007).
[11] T. Nash *et al.*, Physics of Plasmas **11**, L65 (2004).
[12] M. D. Knudson, R. Lemke, D. Hayes, C. A. Hall, C. Deeney, and J. Asay, Journal of Applied Physics **94**, 4420 (2003).
[13] V. I. Oreshkin, S. A. Chaikovskii, N. A. Labetskaya, Y. F. Ivanova, K. V. Khishchenko, P. R. Levashov, N. I. Kuskova, and A. D. Rud, Technical Physics **57**, 198 (2012).
[14] T. Awe, B. Bauer, S. Fuelling, I. Lindemuth, and R. Siemon, Physics of Plasmas **17**, 102507 (2010).
[15] T. Awe, E. Yu, K. Yates, W. Yelton, B. Bauer, T. Hutchinson, S. Fuelling, and B. Mckenzie, IEEE Transactions on plasma science **45**, 584 (2017).
[16] S. Chaikovsky, V. I. Oreshkin, G. Mesyats, N. A. Ratakhin, I. Datsko, and B. Kablambaev, Physics of Plasmas **16**, 042701 (2009).
[17] S. Chaikovsky, V. I. Oreshkin, I. Datsko, N. Labetskaya, D. Rybka, and N. A. Ratakhin, Physics of Plasmas **22**, 112704 (2015).
[18] V. I. Oreshkin and R. B. Baksht, IEEE Transactions on Plasma Science **48**, 1214 (2020).
[19] V. I. Oreshkin, R. Baksht, N. A. Ratakhin, A. V. Shishlov, K. Khishchenko, P. Levashov, and I. Beilis, Physics of Plasmas **11**, 4771 (2004).
[20] R. Baksht, A. Rousskikh, A. Zhigalin, V. I. Oreshkin, and A. Artyomov, Physics of Plasmas **22**, 103521 (2015).
[21] V. Oreshkin, S. Chaikovsky, I. Datsko, N. Labetskaya, G. Mesyats, E. Oreshkin, N. Ratakhin, and D. Rybka, Physics of Plasmas **23**, 122107 (2016).
[22] I. Datsko, N. Labetskaya, S. Chaikovsky, V. Van'kevich, and V. Oreshkin, Journal of Physics: Conference Series **2064**, 012012 (2021).
[23] A. Kim, B. Kovalchuk, V. Kokshenev, A. Shishlov, N. Ratakhin, V. Oreshkin, V. Rostov, V. Koshelev, and V. Losev, Matter and Radiation at Extremes **1**, 201 (2016).
[24] B. Kadomtsev, *Reviews of Plasma Physics* (Consultants Bureau, New York, 1980), Vol. 2.
[25] V. I. Oreshkin, Physics of Plasmas **15**, 092103 (2008).
[26] A. Rousskikh, V. I. Oreshkin, S. Chaikovsky, N. Labetskaya, A. V. Shishlov, I. Beilis, and R. Baksht, Physics of Plasmas **15**, 102706 (2008).
[27] P. Kubes *et al.*, Physics of Plasmas **24**, 032706 (2017).
[28] P. Kubes, M. Paduch, J. Cikhardt, J. Kortanek, B. Cikhardtova, K. Rezac, D. Klir, J. Kravarik, and E. Zielinska, Physics of Plasmas **21**, 122706 (2014).
[29] V. Oreshkin, R. Baksht, E. Oreshkin, A. Rousskikh, and A. Zhigalin, Plasma Physics and Controlled Fusion **62**, 035016 (2020).

[30] V. Oreshkin and E. Oreshkin, Plasma Physics and Controlled Fusion **63**, 125013 (2021).
[31] G. A. Mesyats, IEEE Transactions on plasma science **23**, 879 (1995).
[32] S. P. Bugaev, E. A. Litvinov, G. A. Mesyats, and D. I. Proskurovskiĭ, Soviet Physics Uspekhi **18**, 51 (1975).
[33] G. A. Mesyats, Physics-Uspekhi **38**, 567 (1995).
[34] G. Mesyats, *Pulsed power engineering and electronics* (Nauka, Moscow, 2004).
[35] A. Samokhin, Plasma physics reports **36**, 149 (2010).
[36] V. Oreshkin, S. Chaikovsky, and E. Oreshkin, in *Journal of Physics: Conference Series* (IOP Publishing, 2021), p. 012018.
[37] E. Oreshkin, S. Barengolts, G. Mesyats, V. Oreshkin, and K. Khishchenko, Journal of Physics: Conference Series **774**, 012191 (2016).
[38] S. A. Barengolts, V. G. Mesyats, V. I. Oreshkin, E. V. Oreshkin, K. V. Khishchenko, I. V. Uimanov, and M. M. Tsventoukh, Physical Review Accelerators and Beams **21**, 061004 (2018).
[39] G. A. Mesyats and I. V. Uimanov, IEEE Transactions on plasma science **43**, 2241 (2015).
[40] A. Anders and G. Y. Yushkov, Journal of Applied Physics **91**, 4824 (2002).
[41] S. Braginskii, Reviews of plasma physics **1**, 205 (1965).
[42] V. I. Oreshkin, S. A. Barengol'ts, and S. A. Chaikovsky, Technical Physics **52**, 642 (2007).
[43] S. I. Tkachenko, K. V. Khishchenko, V. S. Vorob'ev, P. R. Levashov, I. V. Lomonosov, and V. E. Fortov, High Temperature **39**, 674 (2001).
[44] A. Bushman and V. Fortov, Sov. Tech. Rev. B **1**, 219 (1987).
[45] M. P. Desjarlais, Contributions to Plasma Physics **41**, 267 (2001).
[46] Y. T. Lee and R. More, The Physics of fluids **27**, 1273 (1984).
[47] V. I. Oreshkin and S. Chaikovsky, Physics of Plasmas **19**, 022706 (2012).
[48] S. Krivosheev, V. Pomazov, and G. Shneerson, Technical Physics Letters **37**, 877 (2011).
[49] L. D. Landau, J. Bell, M. Kearsley, L. Pitaevskii, E. Lifshitz, and J. Sykes, *Electrodynamics of continuous media* (Elsevier, 1984), Vol. 8.
[50] D. Mikitchuk, C. Stollberg, R. Doron, E. Kroupp, Y. Maron, H. R. Strauss, A. L. Velikovich, and J. L. Giuliani, IEEE Transactions on Plasma Science **42**, 2524 (2014).
[51] A. Rousskikh, A. Zhigalin, V. I. Oreshkin, V. Frolova, A. Velikovich, G. Y. Yushkov, and R. Baksht, Physics of Plasmas **23**, 063502 (2016).
[52] D. Yanuka, A. Rososhek, S. Theocharous, S. Bland, Y. E. Krasik, M. Olbinado, A. Rack, and E. Oreshkin, Physics of Plasmas **26**, 050703 (2019).

Journal of Applied Physics



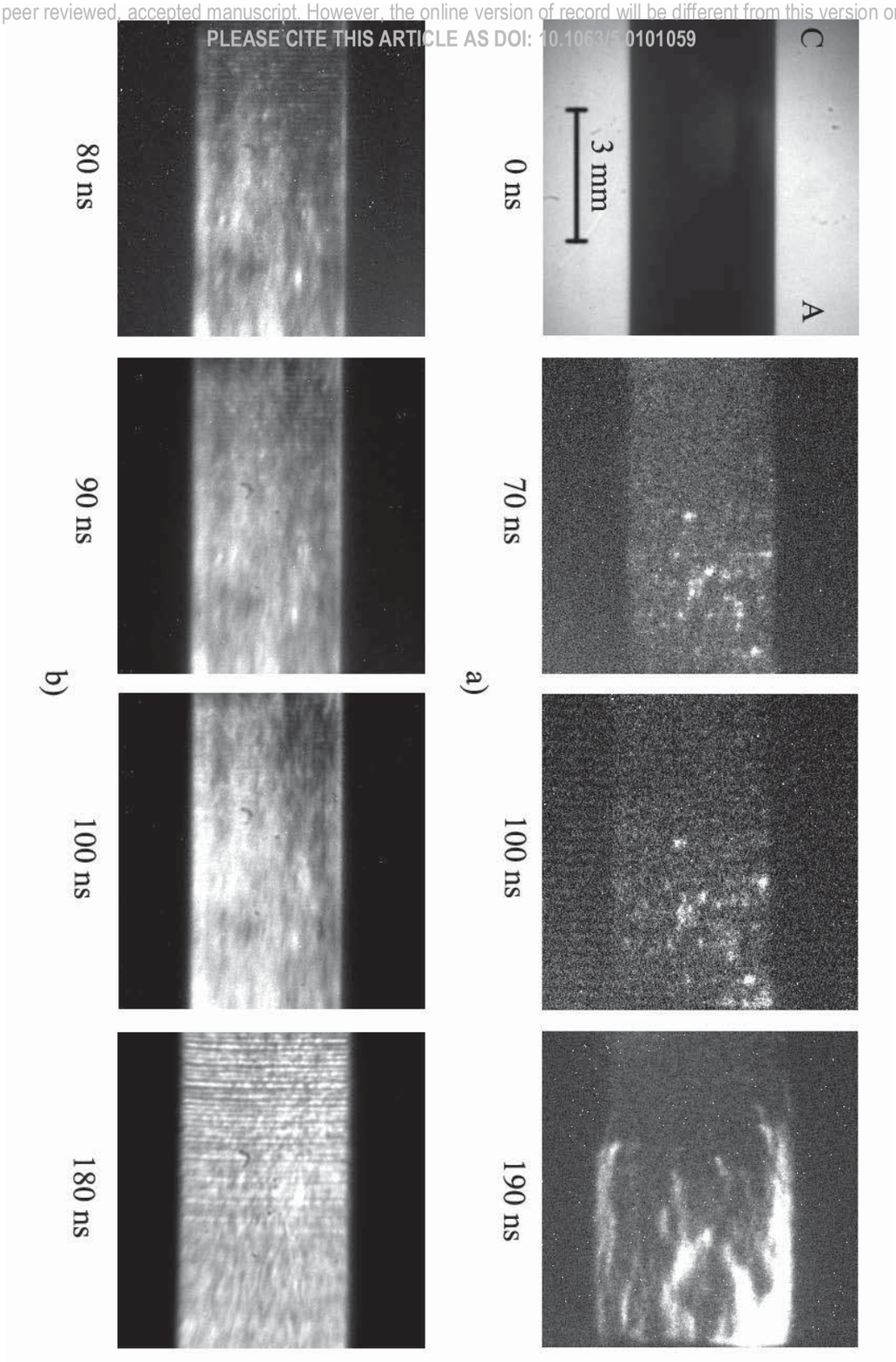

AIP Publishing
Journal of Applied Physics
ACCEPTED MANUSCRIPT


PLEASE CITE THIS ARTICLE AS DOI: 10.1063/5.0101059

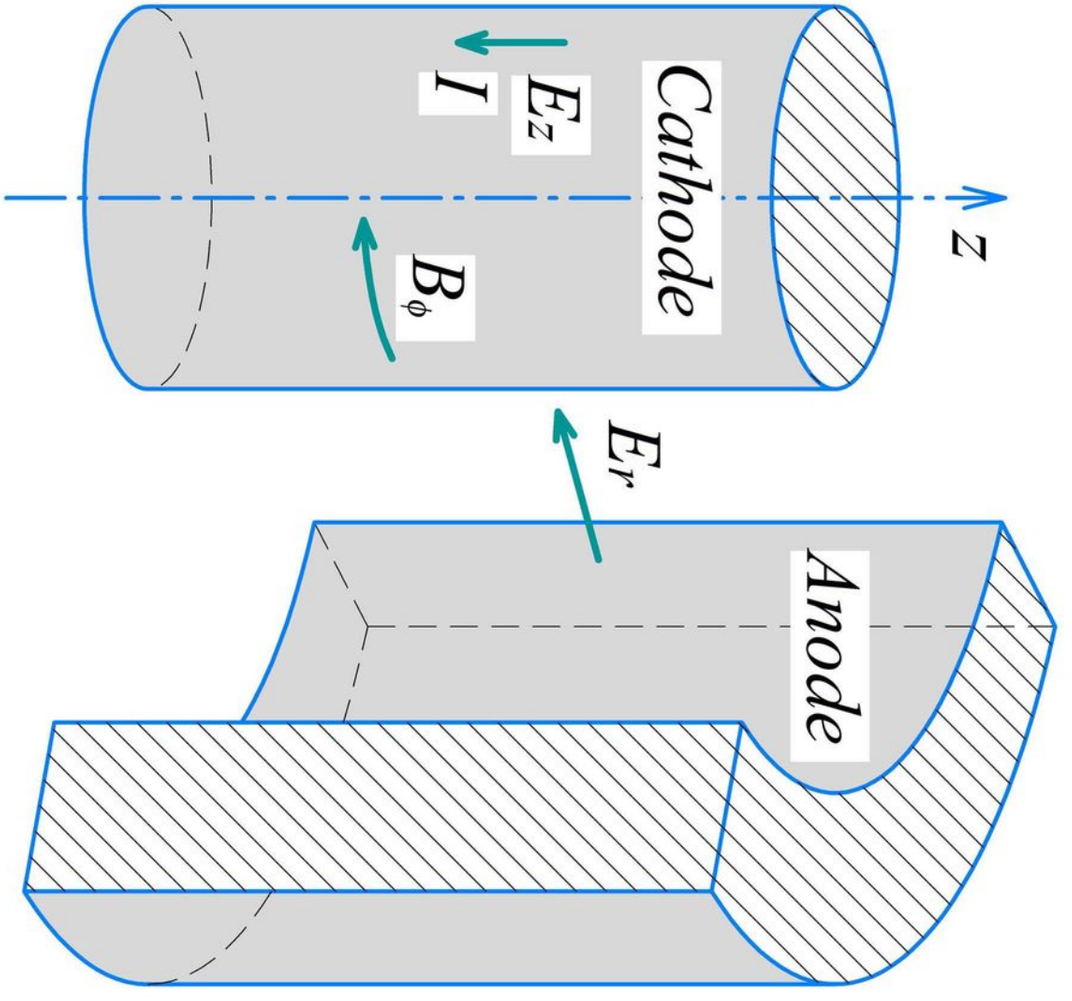

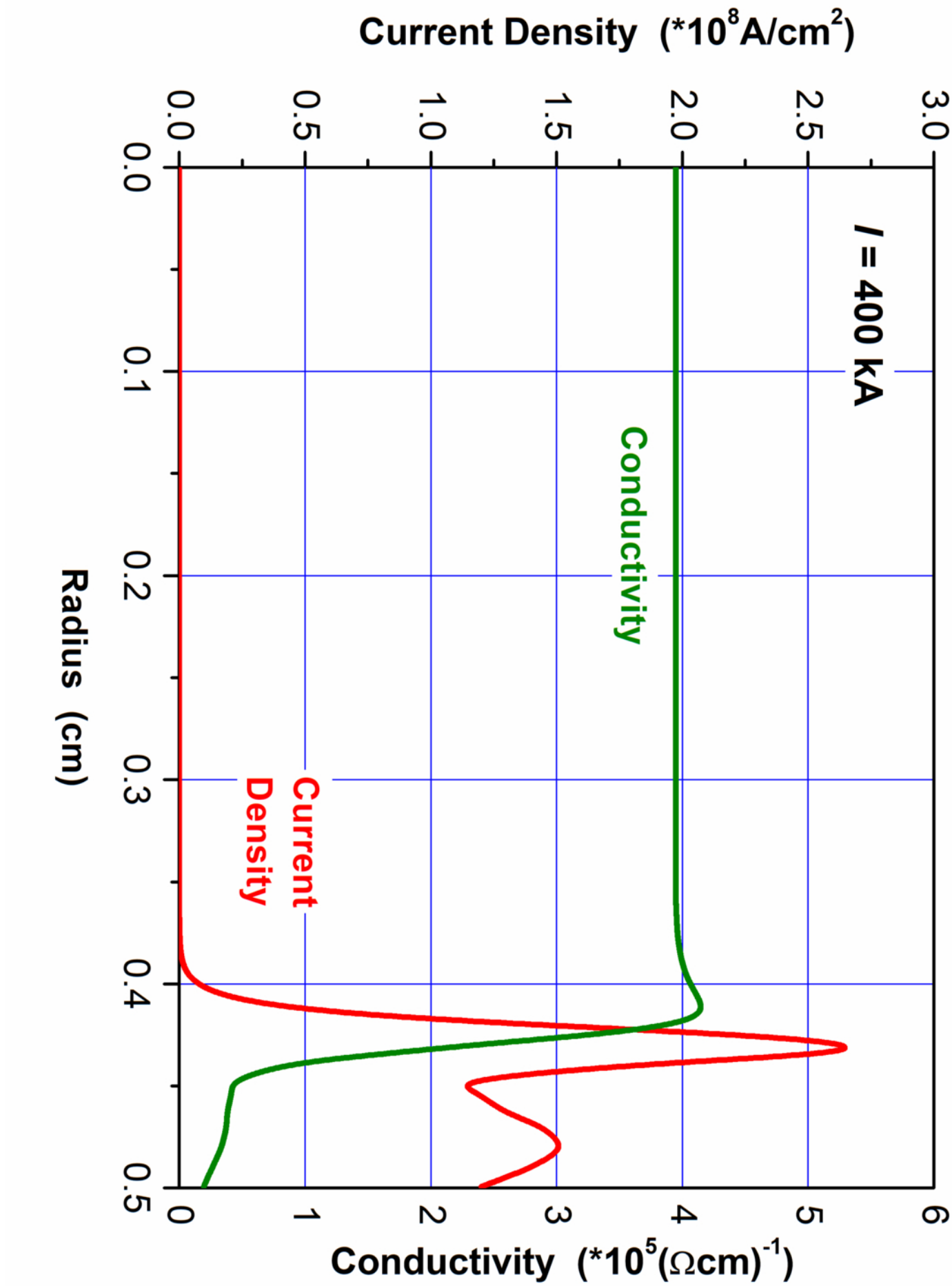

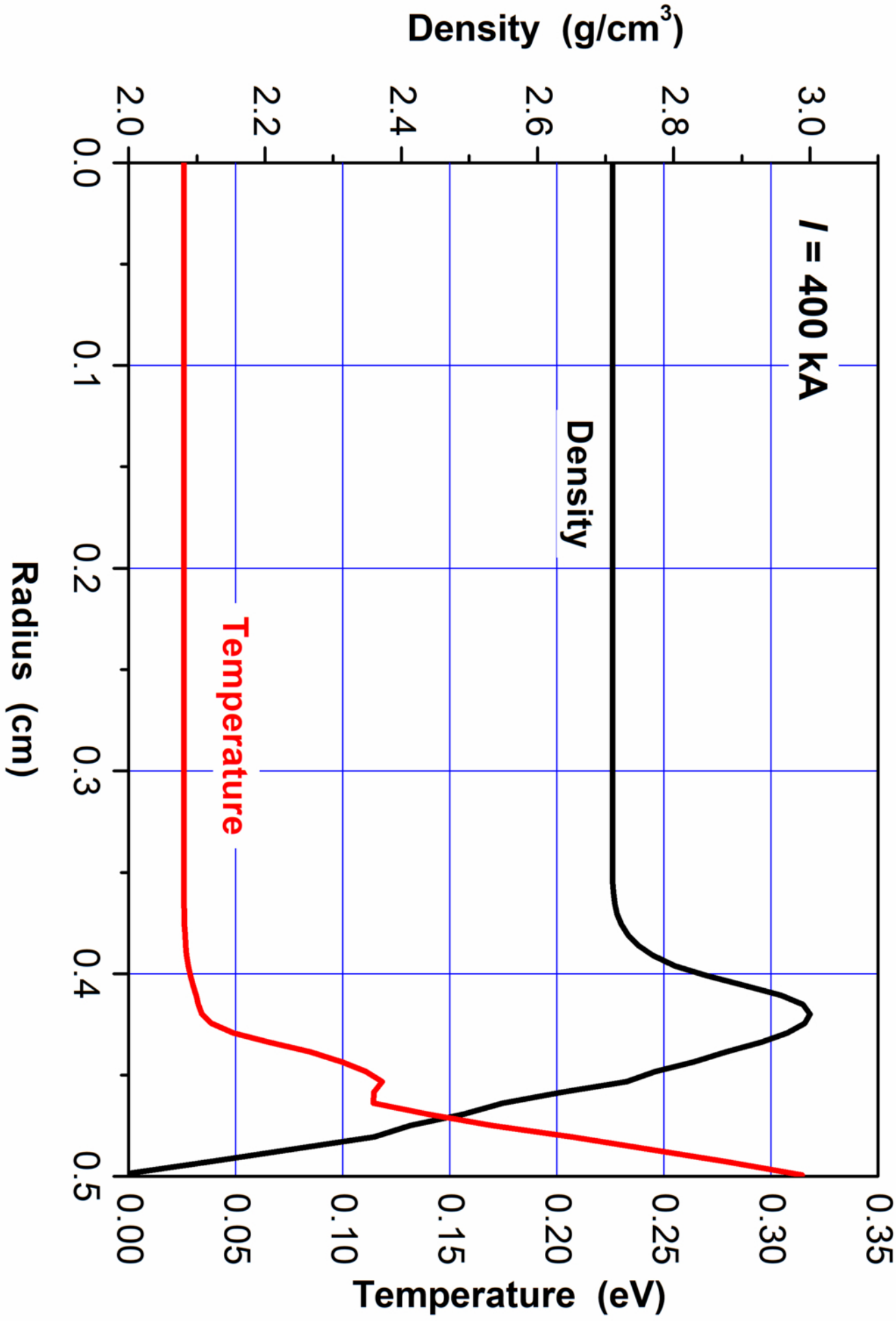

Journal of Applied Physics


PLEASE CITE THIS ARTICLE AS DOI: 10.1063/5.0101059

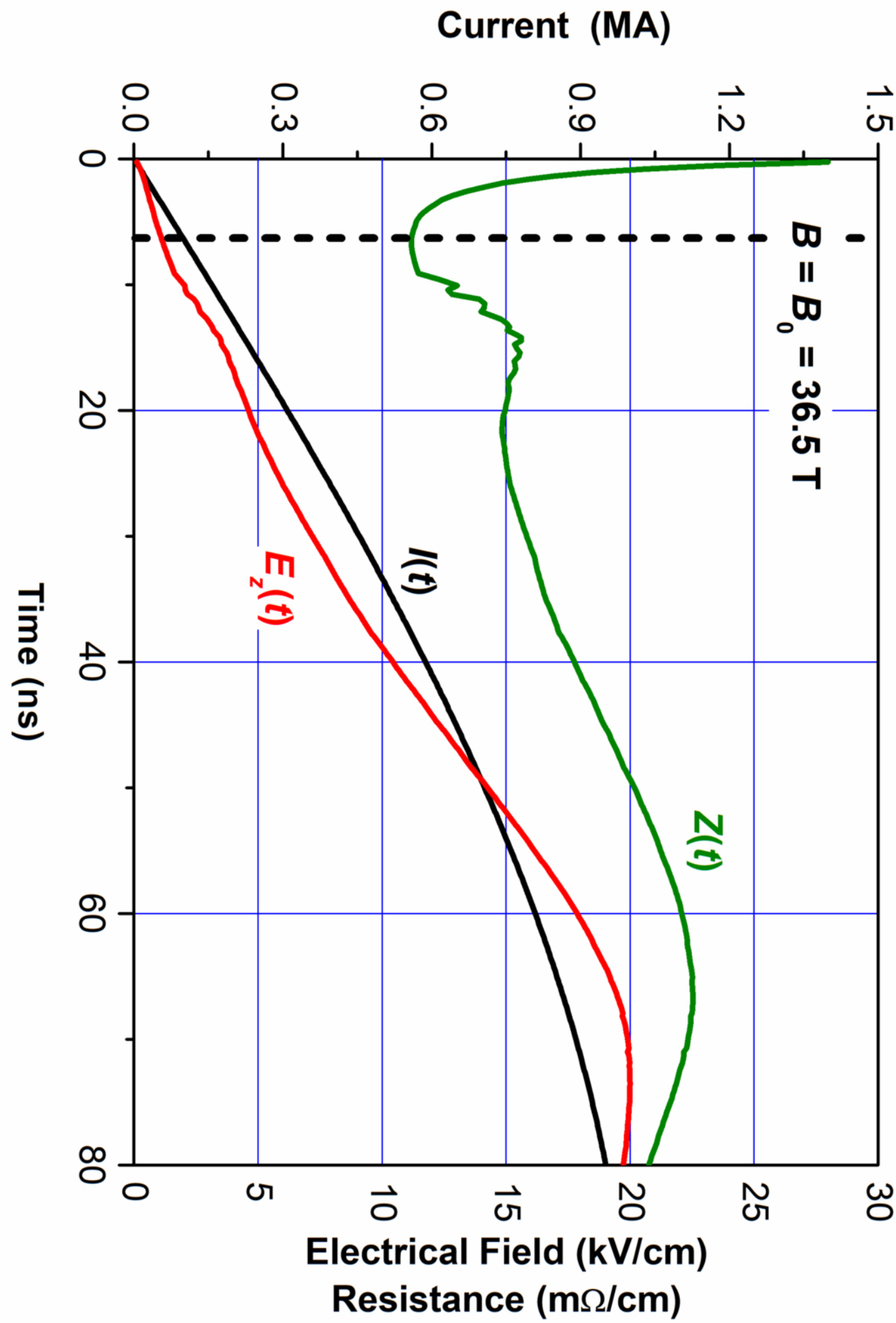

Journal of Applied Physics


PLEASE CITE THIS ARTICLE AS DOI: 10.1063/5.0101059